Model simulations of global change in the ionosphere

Liying Qian,[1] Stanley C. Solomon,[1] Raymond G. Roble,[1] and Timothy J. Kane[2]

Received 31 December 2007; revised 17 February 2008; accepted 7 March 2008; published 5 April 2008.

[1] Observations of secular trends in the E and F_1 regions of the ionosphere indicate that electron densities have increased, and that the height of the E-region peak has decreased, during the past several decades. Detection of trends in the upper ionosphere through analysis of F_2-layer parameters has been more complex and controversial. In order to facilitate observational detection of long-term trends in the ionosphere, simulations were performed using a single-column upper atmosphere model. CO_2 concentrations for the year 2000 and projected for the year 2100 were used to investigate changes of electron densities and the altitudes of ionospheric layers. Results show that increased CO_2 concentration increases electron density in the lower regions of the ionosphere, but decreases electron density in the upper ionosphere. The transition altitude occurs slightly below the F_2 peak altitude (h_mF_2). The proximity of h_mF_2 to the transition altitude may explain why different analyses of long-term trends in F_2 peak density have shown both positive and negative trends. The altitudes of the E, F_1 and F_2 regions all decrease with increased CO_2 concentration.
Citation: Qian, L., S. C. Solomon, R. G. Roble, and T. J. Kane (2008), Model simulations of global change in the ionosphere, *Geophys. Res. Lett.*, *35*, L07811, doi:10.1029/2007GL033156.

1. Introduction

[2] *Roble and Dickinson* [1989] first suggested that there would be long-term changes of the ionospheric E- and F-region peak densities in response to cooling and contraction of the mesosphere and the thermosphere, due to changes in greenhouse gas concentrations. *Rishbeth* [1990] concluded that long-term cooling in the upper atmosphere would lower the E- and F_2-region peak heights but that changes in the E- and F_2-region electron density should be small. *Rishbeth and Roble* [1992] investigated global change in the ionosphere using the NCAR Thermosphere-Ionosphere General Circulation Model (TIGCM) [*Roble et al.*, 1988] by doubling CO_2 and CH_4 concentrations, and found that the height of the F_2-layer peak dropped on average by about 15 km but that the F_2-layer electron density change was minimal. Following these theoretical and modeling studies, ground-based ionosonde data have been analyzed in attempts to detect long-term trends in the ionosphere [e.g., *Bremer*, 1992; *Ulich and Turunen*, 1997; *Bremer*, 1998; *Upadhyay and Mahajan*, 1998; *Danilov and Mikhailov*, 1999; *Mikhailov and Marin*, 2000, 2001; *Clilverd et al.*, 2003; *Danilov*, 2003]. There is evidence that the altitudes of the E and F_1 regions have decreased, and that the E- and F_1-region electron densities have increased in the past three to four decades [*Bremer*, 1998, 2001; *Laštovička and Bremer*, 2004; *Laštovička et al.*, 2006a]. Detection of long-term trends of F_2 parameters has been more complex and controversial with regard to methodology, results, and interpretation [*Bremer*, 1998; *Mikhailov and Marin*, 2000, 2001; *Danilov*, 2001; *Clilverd et al.*, 2003; *Danilov*, 2003; *Laštovička*, 2005; *Laštovička et al.*, 2006a, 2006b]. Both negative and positive trends of F_2 peak electron density have been inferred; long-term changes of geomagnetic activity and greenhouse gas concentrations have been invoked as explanations.

[3] Causes of long-term trends of the ionosphere can be natural or anthropogenic in origin [*Rishbeth*, 1997]. Long-term changes in solar activity and geomagnetic activity could cause secular change in the ionosphere. Trends in the neutral atmosphere [*Keating et al.*, 2000; *Emmert et al.*, 2004; *Marcos et al.*, 2005], which have been mainly attributed to increased concentration of CO_2, can cause changes in the ionosphere through production, loss, and transport of the plasma. In addition, F_2 region of the ionosphere is strongly influenced by dynamics and electrodynamics. Neutral winds or electric fields can shift the F_2 peak altitude and change its density, and thus can cause complex geographic and solar local time distributions of any long-term trends.

[4] The purpose of this study is to explore mechanisms of trends in the ionosphere, to explain the complex pattern and controversies found in observations of trends of F_2 parameters, and to facilitate ionosonde data analysis of long-term trends. Although secular trends in the past several decades may be influenced by natural causes, observed trends in the upper atmosphere and ionosphere have been mainly attributed to the steady increase of greenhouse gas concentrations [*Danilov*, 2003; *Laštovička*, 2005]. Therefore, this study focuses on investigation of ionospheric trends due to increased concentration of the greenhouse gas CO_2. Long-term trends in the E and lower F_1 regions may be slightly affected by stratosphere ozone depletion since the effect of ozone depletion on lower thermospheric temperature and density has been demonstrated by model study [*Akmaev et al.*, 2006]. However, this secondary effect is not treated here. This paper addresses long-term trends of the global mean ionosphere rather than global distributions of the trends, and physical processes in the ionosphere are invoked to explain the changes in different ionospheric regions.

2. Model Description

[5] The model used in these studies is a self-consistent global mean model of the mesosphere, the thermosphere, and the ionosphere. Its original version is described by *Roble et al.* [1987]; extension to the mesosphere and additional modifications are documented by *Roble* [1995].

[1]High Altitude Observatory, National Center for Atmospheric Research, Boulder, Colorado, USA.
[2]Department of Electrical Engineering and Department of Meteorology, Pennsylvania State University, University Park, Pennsylvania, USA.

0094-8276/08/2007GL033156$05.00

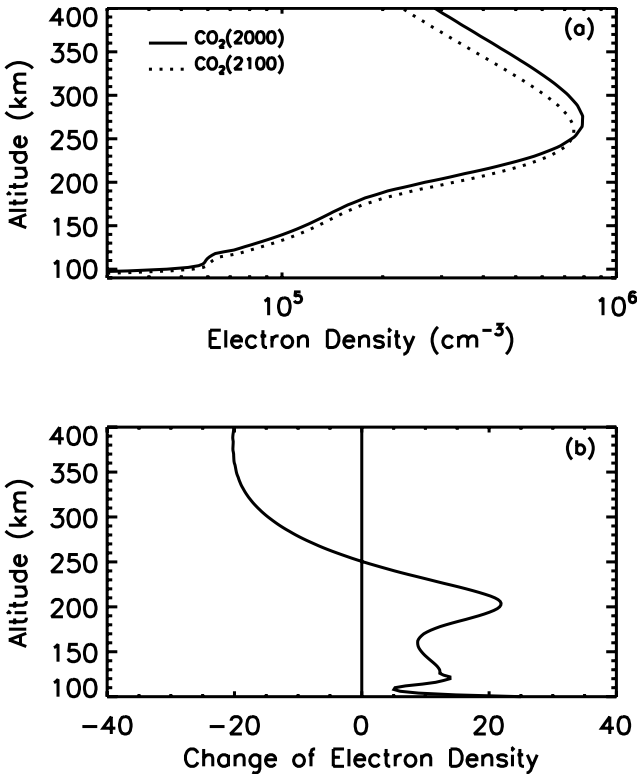

Figure 1. (a) Electron number density profiles for the base case and the doubled CO_2 case, under solar medium conditions ($F_{10.7} = \overline{F}_{10.7} = 150$). Solid line, base case; dotted line, doubled CO_2 case. (b) Percentage change of electron number density from the doubled CO_2 case to the base case, under solar medium conditions ($F_{10.7} = \overline{F}_{10.7} = 150$).

The model is a 1D representation of aeronomic processes in the NCAR Thermosphere-Ionosphere-Mesosphere-Electrodynamic General Circulation Model (TIME-GCM) [*Roble and Ridley*, 1994], and can be considered the single-column version of the TIME-GCM. Recent improvements include incorporation of a new solar EUV energy deposition scheme [*Solomon and Qian*, 2005], and updates to cooling rates and odd-nitrogen chemistry [*Roble and Solomon*, 2005].

[6] For present-day simulations, the model was run to steady state with a CO_2 concentration of 365 ppmv imposed at the lower boundary (30 km), representative of the year 2000. For a future projection, a CO_2 concentration of 730 ppmv was applied at the lower boundary, representative of the year 2100, as projected by the *Intergovernmental Panel on Climate Change (IPCC)* [2007] emission scenario A1B, a medium emission scenario. Different solar activity levels were employed but low geomagnetic activity conditions were assumed. Electron density profiles obtained by the different model experiments were then compared to quantify changes of ionospheric parameters. Mechanisms of these changes were explored, and solar-cycle dependence of these changes was also investigated.

3. Results

3.1. Long-term Trends in the E, F_1, and F_2 Regions

[7] In response to cooling and contraction of the middle atmosphere and thermosphere, the entire ionosphere will similarly contract, leading to lower altitudes of the E-region and F-region density peaks h_mE and h_mF_2. Changes in the magnitudes of the density peaks N_mE and N_mF_2, and changes in density throughout the ionosphere, are more subtle. Model experiments assuming moderate levels of solar activity ($F_{10.7}$ = 150) were conducted to illustrate these changes.

[8] Figure 1a shows electron density profiles with CO_2 concentrations at year 2000 level and the projected year 2100 level. The altitudes of the E and F_1 regions decrease, which is consistent with the cooling and contraction of the thermosphere, while their electron density increases. Increase of electron density in the E- and F_1-region electron density is controlled by compositional changes and subsequent changes in photochemical equilibrium. Section 3.2 provides a detailed discussion of the mechanisms. This pattern of decrease of altitude and increase of electron density in the lower ionosphere agrees with results from ionosonde data analyses [*Bremer*, 1998, 2001; *Laštovička and Bremer*, 2004; *Laštovička et al.*, 2006a].

[9] The F_2 region contains both positive and negative change regions, but the peak electron density N_mF_2 decreases with increased CO_2 forcing. The transition altitude from positive change to negative change is near but slightly below the peak altitude h_mF_2. This altitude indicates a transition from control by photochemical equilibrium to plasma transport, as discussed in section 3.2. Changes in forcing of photochemical equilibrium or forcing of transport can potentially cause a shift in this altitude. The proximity of the positive-to-negative transition to h_mF_2 may explain why ionosonde data analyses have resulted in a complex pattern of long-term trends in F_2 peak electron density, with both positive and negative trends detected. Recent reviews of long-term trends of F_2 peak electron density by *Laštovička et al.* [2006b, 2008] concluded that long-term trends of N_mF_2 are either negative or insignificant. This pattern of long-term trends of N_mF_2 is consistent with these model simulations. Figure 1a also shows that the altitude of the F_2 region, including h_mF_2, decreases with increased CO_2 concentration.

3.2. Mechanisms of Global Change in the Ionosphere

[10] The model experiments described in section 3.1 were analyzed to elucidate the reasons for the changes shown in Figure 1. The increased CO_2 concentration causes electron density increases in the lower ionosphere up to about 250 km; above that altitude, electron density decreases. To understand the causes of this transition, simplified physics of the quasi-equilibrium ionosphere are described below.

[11] Electron density in the E region is proportional to ionization rate but inversely proportional to the ratio of the two major ions in the E region, NO^+ and O_2^+. The E region is in approximate photochemical equilibrium between photoionization and loss of ions through dissociative recombination:

$$M_2 + h\nu \xrightarrow{q} M_2^+ + e \qquad M_2^+ + e \xrightarrow{\alpha} M + M$$

where M_2 represents major species in the E region, which are O_2 and N_2, q is the ionization rate, and α is the effective dissociative recombination rate. Since N_2^+ is rapidly converted to NO^+ and O_2^+ through reactions with atomic and

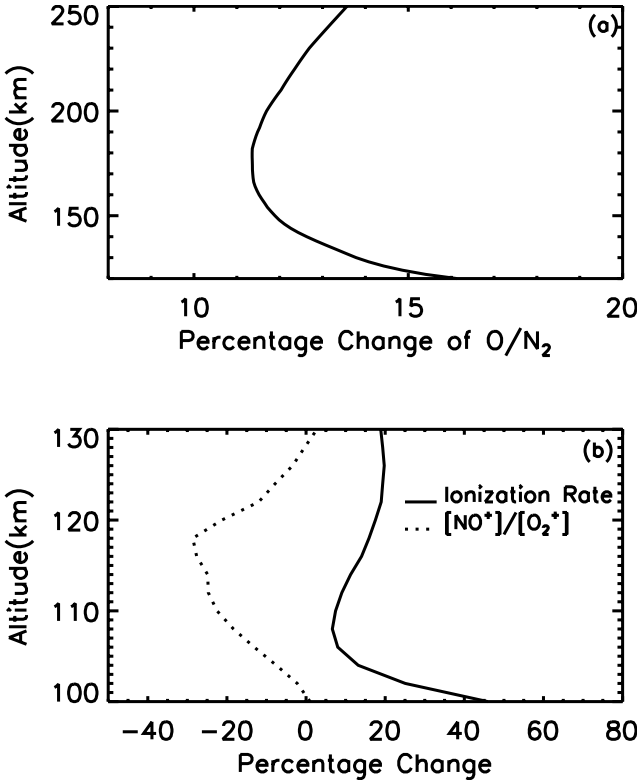

Figure 2. (a) Percentage change of O/N_2 from the base case to the doubled CO_2 case in the altitude range 120 km to 250 km, under solar medium conditions ($F_{10.7} = \overline{F}_{10.7} = 150$). (b) Percentage changes from the base case to the doubled CO_2 case for the total ionization rate and the ratio of NO^+ number density to O_2^+ number density in the E region, under solar medium conditions ($F_{10.7} = \overline{F}_{10.7} = 150$).

molecular oxygen, the major ions in the E region are NO^+ and O_2^+. Assuming photochemical equilibrium, $q = \alpha[M_2^+][e]$, where $[M_2^+]$ and $[e]$ are ion and electron number density, respectively. Assuming charge neutrality, $[e] = \left(\frac{q}{\alpha}\right)^{1/2}$. Since the dissociative recombination rate of NO^+ is nearly twice that of O_2^+, the effective recombination rate α is proportional to NO^+/O_2^+, and electron density is inversely proportional to this ratio:

$$[e] \propto q/\left([NO^+]/[O_2^+]\right)$$

[12] Figure 2b shows the corresponding altitude profile of percentage changes of the ionization rate and the ratio of NO^+ and O_2^+ from year 2000 to year 2100, between 100 km and 130 km. Change of the ratio of NO^+ to O_2^+ is negative in the E region. This is because lower temperature due to increased CO_2 concentration causes lower NO density, which in turn decreases NO^+ density since the main source of NO^+ is the reaction of O_2^+ with NO. Possible negative secular trends of NO^+/O_2^+ in the E region have been observed [*Danilov*, 1997, 2001]. Change of the ionization rate is positive at all E-region altitudes. Cooling and contraction of the thermosphere causes less absorption of solar irradiance before it reaches E-region altitudes, and thus enhances ionization rates in this region. Consequently, electron density in this altitude range increases with increasing CO_2 concentration.

[13] As the ionosphere transitions from the E region to the F region, atomic oxygen becomes the major neutral species. The F region up to the F_2 peak is also in approximate photochemical equilibrium, but different photochemical production and loss processes dominate. The production of ions is mostly due to ionization of atomic oxygen. Since the recombination rate of O^+ is slow, loss of ions goes through two steps: transfer of O^+ to NO^+ and O_2^+ through atom-ion interchange reactions followed by dissociative recombination of the molecular ions. The atom-ion interchange reactions are much slower than the dissociative recombination rates. Consequently, electron density is determined by the balance between the ionization rate and the rates of the atom-ion interchange reactions. Since N_2 dominates over O_2, electron density is roughly proportional to the ratio of O and N_2, i.e., $[e] \propto O/N_2$. Figure 2a shows altitude profile of percentage change of O/N_2 from 2000 to 2100 scenario in this region. Change of O/N_2 is positive (on constant altitude surfaces) due to the cooling and contraction of the atmosphere, which yields an increase in electron density.

[14] The F_2 peak occurs where transport of the plasma becomes comparable to chemical production and loss. Above the F_2 peak, the electron density altitude profile becomes mainly controlled by plasma transport. Consequently, electron density decreases exponentially with the plasma scale height. Since the cooling and thus contraction of the atmosphere reduces the plasma scale height, electron density decreases responding to increased CO_2 concentration in this altitude range.

3.3. Solar Cycle Dependence of Ionospheric Changes

[15] Thermospheric long-term trends show a clear solar-cycle dependence, with the secular decrease of neutral density under solar minimum conditions approximately three times of that under solar maximum conditions [*Emmert et al.*, 2004; *Qian et al.*, 2006]. It is reasonable to expect that the ionospheric long-term trends will also depend on solar activity. This was investigated using model experiments with CO_2 concentrations for 2000 and 2100 as projected by the *IPCC* [2007] A1B emission scenario, under solar minimum and solar maximum conditions ($F_{10.7}$ = 70, 200). Table 1 shows changes of E- and F_2-region parameters as a result of increased CO_2 concentration from 2000 to 2100. h_mF_2 decreases by 14 km and 10 km under solar minimum and solar maximum conditions, respectively, while N_mF_2 decreases by 9% and 4%. Therefore, trends of F_2 parameters are expected to be larger under solar minimum conditions, similar to the solar-cycle dependence

Table 1. Changes of Ionospheric Parameters Due to Change of CO_2 Concentration From 2000 to the Projected 2100 Concentration Based on the IPCC Emission Scenario A1B, Under Solar Minimum and Solar Maximum Conditions

	Solar Min	Solar Max
h_mF_2	−14 km	−10 km
N_mF_2	−9%	−4%
h_mE	−2 km	−4 km
N_mE	+4%	+2%

of secular change in the thermosphere. h_mE decreases 2 km under solar minimum conditions and 4 km under solar maximum conditions. Changes of N_mE are relatively small, with 4% and 2% increases under solar minimum and solar maximum, respectively.

4. Discussion

[16] Model experiments show that long-term trends of electron density transitions from positive at lower altitudes to negative at higher altitudes responding to increased CO_2 concentrations; the transition altitude is near but below the F_2 peak. The positive and negative trends are determined by basic ionospheric physics, with positive trends in altitude ranges governed by photochemical equilibrium, and negative trends at higher altitude where plasma transport dominates.

[17] The E and F_1 regions are within the positive change range and thus electron density in these regions should increase with increasing CO_2 concentration. The E-region peak altitude, however, should decrease with increased CO_2 concentration. This pattern of increase of electron density and decrease of the altitude of the lower ionosphere is consistent with results from analyses of ionosonde data attempting to measure long-term trends in the E and F_1 regions during the past several decades. The F_2 region consists of both positive and negative change regions, with the transition altitude near the F_2 peak altitude. This may explain the complex results obtained from different analyses of ionosonde observations of secular change in F_2 peak electron density, with both positive and negative trends found. Model simulation of the F_2 peak electron density predicts that it decreases with increased CO_2 concentration, in agreement with recent reviews of ionosonde trend detection. These simulations show that the F_2 peak altitude also decreases with increased CO_2 concentration.

[18] Trends in ionospheric F_2 parameters are larger under solar minimum conditions than solar maximum conditions, similar to the solar-cycle dependence of secular trends in the thermosphere. This can be explained by examining the effects of stronger cooling under solar minimum conditions. The larger temperature decrease due to doubling of CO_2 under solar minimum conditions causes a larger decrease in plasma scale height, which in turn causes a fixed pressure surface to descend more compared to the case of solar maximum conditions. Since h_mF_2 tends to remain on the same pressure surface as temperature changes [*Garriott and Rishbeth*, 1963], h_mF_2 will have a larger decrease under solar minimum conditions. In addition, the F_2 peak is where chemical control of plasma density gives way to transport control. Plasma transport causes plasma density to decrease according to plasma scale height. Therefore, a larger change in plasma scale height under solar minimum conditions can result in greater change in N_mF_2.

[19] These results may give some guidance to further analyses of long-term ionospheric measurements. Changes in h_mE may be a significant fraction of a scale height in the E-region, but since scale heights are low at these altitudes, this may be difficult to measure on decadal periods. Changes in N_mE are small but detectable [*Bremer*, 2001; *Bremer et al.*, 2004]. The secular trends in N_mF_2 may be comparatively small compared to intrinsic variability in the F-region, but this parameter is the most unambiguous and stable measurement that can be obtained from the extensive ionosonde historical data set, and is worth tracking carefully. The accurate measurement of h_mF_2 may be more difficult using ionosonde measurements, but it is obtainable from incoherent scatter radar observations, and it is the most direct and significant secular change that is expected from increasing CO_2 levels.

[20] The upper ionosphere is highly influenced by neutral atmosphere dynamics and by electrodynamics. These effects could cause significant regional features in F_2 long-term trends. For instance, long-term changes in the geomagnetic field could significantly influence secular change in the ionosphere in some geographic regions. Just as simulations of climate in the troposphere and at the Earth's surface are progressing from general averages of expected changes to regional climate change, studies of the effects in the thermosphere/ionosphere system must similarly progress. Three-dimensional modeling studies may improve our interpretation and understanding of secular trends inferred at particular geographic locations.

[21] **Acknowledgments.** This research was supported by NASA grants NNX07AC55G, NNX07AC61G, and NNH05AB55I to the National Center for Atmospheric Research. NCAR is supported by the National Science Foundation.

References

Akmaev, R. A., V. I. Fomichev, and X. Zhu (2006), Impact of middle-atmospheric composition changes on greenhouse cooling in the upper atmosphere, *J. Atmos. Terr. Phys.*, *68*, 1879–1889.

Bremer, J. (1992), Ionospheric trends in mid-latitudes as a possible indicator of the atmospheric greenhouse effect, *J. Atmos. Terr. Phys.*, *54*, 1505–1511.

Bremer, J. (1998), Trends in the ionospheric E and F regions over Europe, *Ann. Geophys.*, *16*, 986–996.

Bremer, J. (2001), Trends in the thermosphere derived from global ionosonde observations, *Adv. Space Res.*, *28*, 997–1006.

Bremer, J., L. Alfonsi, P. Bencze, J. Laštovička, A. V. Mikhailov, and N. Rogers (2004), Long-term trends in the ionosphere and upper atmosphere parameters, *Ann. Geophys.*, *47*, 1009–1029.

Clilverd, M. A., T. Ulich, and M. J. Jarvis (2003), Residual solar cycle influence on trends in ionospheric F2–layer peak height, *J. Geophys. Res.*, *108*(A12), 1450, doi:10.1029/2003JA009838.

Danilov, A. D. (1997), Long-term changes of the mesosphere and lower thermosphere temperature and composition, *Adv. Space Res.*, *20*, 2137–2147.

Danilov, A. D. (2001), Do ionospheric trends indicate to the greenhouse effect?, *Adv. Space Res.*, *28*, 987–996.

Danilov, A. D. (2003), Long-term trends in foF2 independent of geomagnetic activity, *Ann. Geophys.*, *21*, 1167–1176.

Danilov, A. D., and A. V. Mikhailov (1999), Spatial and seasonal variations of the foF2 long-term trends, *Ann. Geophys.*, *17*, 1239–1243.

Emmert, J. T., J. M. Picone, J. L. Lean, and S. H. Knowles (2004), Global change in the thermosphere: Compelling evidence of a secular decrease in density, *J. Geophys. Res.*, *109*, A02301, doi:10.1029/2003JA010176.

Garriott, O. K., and H. Rishbeth (1963), Effects of temperature changes on the electron density profile in the F_2 layer, *Planet. Space Sci.*, *11*, 587–590.

Intergovernmental Panel on Climate Change (IPCC) (2007), *Climate Change 2007: The Physical Science Basis*, edited by S. Solomon, Cambridge Univ. Press, Cambridge, U. K.

Keating, G. M., R. H. Tolson, and M. S. Bradford (2000), Evidence of long-term global decline in the Earth's thermospheric densities apparently related to anthropogenic effects, *Geophys. Res. Lett.*, *27*, 1523–1526.

Laštovička, J. (2005), On the role of solar and geomagnetic activity in long-term trends in the atmosphere-ionosphere system, *J. Atmos. Terr. Phys.*, *67*, 83–92.

Laštovička, J., and J. Bremer (2004), An overview of long-term trends in the lower ionosphere below 120 km, *Surv. Geophys.*, *25*, 69–99.

Laštovička, J., R. A. Akmaev, G. Beig, J. Bremer, and J. T. Emmert (2006a), Global change in the upper atmosphere, *Science*, *314*, 1253–1254.

Laštovička, J., et al. (2006b), Long-term trends in foF2: A comparison of various methods, *J. Atmos. Terr. Phys.*, *68*, 1854–1870.

Laštovička, J., R. A. Akmaev, G. Beig, J. Bremer, J. T. Emmert, C. Jacobi, M. J. Jarvis, G. Nedoluha, Y. I. Portnyagin, and T. Ulich (2008), Emerging pattern of global change in the upper atmosphere and ionosphere, *Ann. Geophys.*, in press.

Marcos, F. A., J. O. Wise, M. J. Kendra, N. J. Grossbard, and B. R. Bowman (2005), Detection of a long-term decrease in thermospheric neutral density, *Geophys. Res. Lett.*, *32*, L04103, doi:10.1029/2004GL021269.

Mikhailov, A. V., and D. Marin (2000), Geomagnetic control of the foF2 long-term trends, *Ann. Geophys.*, *18*, 653–665.

Mikhailov, A. V., and D. Marin (2001), An interpretation of the foF2 and hmF2 long-term trends in the framework of the geomagnetic control concept, *Ann. Geophys.*, *19*, 733–748.

Qian, L., R. G. Roble, S. C. Solomon, and T. J. Kane (2006), Calculated and observed climate change in the thermosphere, and a prediction for solar cycle 24, *Geophys. Res. Lett.*, *33*, L23705, doi:10.1029/2006GL027185.

Rishbeth, H. (1990), A greenhouse effect in the ionosphere?, *Planet. Space Sci.*, *38*, 945–948.

Rishbeth, H. (1997), Long-term changes in the ionosphere, *Adv. Space Res.*, *20*, 2149–2155.

Rishbeth, H., and R. G. Roble (1992), Cooling of the upper atmosphere by enhanced greenhouse gases: Modeling of thermospheric and ionospheric effects, *Planet. Space Sci.*, *40*, 1011–1026.

Roble, R. G. (1995), Energetics of the mesosphere and thermosphere, in *The Upper Mesosphere and Lower Thermosphere: A Review of Experiment and Theory*, *Geophys. Monogr. Ser.*, vol. 87, edited by R. M. Johnson and T. L. Killeen, pp. 1–22, AGU, Washington, D. C.

Roble, R. G., and R. E. Dickinson (1989), How will changes in carbon dioxide and methane modify the mean structure of the mesosphere and thermosphere?, *Geophys. Res. Lett.*, *16*, 1144–1441.

Roble, R. G., and E. C. Ridley (1994), Thermosphere-ionosphere-mesosphere-electrodynamics general circulation model (TIME-GCM): Equinox solar min simulations, 30–500 km, *Geophys. Res. Lett.*, *21*, 417–420.

Roble, R. G., and S. C. Solomon (2005), On modeling the upper atmosphere and ionosphere response to global change, *Eos Trans. AGU*, *86*(18), Jt. Assem. Suppl., Abstract SA51A-01.

Roble, R. G., E. C. Ridley, and R. E. Dickinson (1987), On the global mean structure of the thermosphere, *J. Geophys. Res.*, *92*, 8745–8758.

Roble, R. G., E. C. Ridley, A. D. Richmond, and R. E. Dickinson (1988), A coupled thermosphere/ionosphere general circulation model, *Geophys. Res. Lett.*, *15*, 1325–1328.

Solomon, S. C., and L. Qian (2005), Solar extreme-ultraviolet irradiance for general circulation models, *J. Geophys. Res.*, *110*, A10306, doi:10.1029/2005JA011160.

Ulich, T., and E. Turunen (1997), Evidence for long-term cooling of the upper atmosphere in ionosonde data, *Geophys. Res. Lett.*, *24*, 1103–1106.

Upadhyay, H. O., and K. K. Mahajan (1998), Atmospheric greenhouse effect and ionospheric trends, *Geophys. Res. Lett.*, *25*, 3375–3378.

T. J. Kane, Department of Electrical Engineering, Pennsylvania State University, University Park, PA 16802, USA.

L. Qian, R. G. Roble, and S. C. Solomon, High Altitude Observatory, National Center for Atmospheric Research, 1850 Table Mesa Dr., Boulder, CO 80307–3000, USA. (lqian@ucar.edu)